Chapter 11
Bioinformatics Insights on Plant Vacuolar Proton Pyrophosphatase: A Proton Pump Involved in Salt Tolerance

Nageswara Rao Reddy Neelapu, Sandeep Solmon Kusuma, Titash Dutta, and Challa Surekha

Contents

11.1 Introduction

Drought, salinity, and extreme temperatures are the major abiotic stress factors that adversely affect plant growth, development, and crop productivity. They alleviate the photosynthetic activity and induce nutrient scarcity and ionic and osmotic stress conditions in plants (Munns and Tester 2008; Rehman et al. 2005; Ashraf et al. 2008).

Salinity leads to degradation of soil fertility as a result of both natural and anthropogenic activities such as irrigation in arid and semiarid regions. Approximately 20% of the irrigated lands, i.e., 45 million hectares, is affected by soil salinization worldwide (Yeo 1999; Munns and Tester 2008). Moreover the change in global climate made rainfall less predictable and caused a drastic shift in the general rainfall pattern. This is of serious concern as there is much decrease in rainfed farm lands which produce one third of the world's food supply.

N. R. R. Neelapu · S. S. Kusuma · T. Dutta · C. Surekha (✉)
Department of Biochemistry and Bioinformatics, Institute of Science, Gandhi Institute of Technology and Management (GITAM) Deemed to be University, Visakhapatnam, AP, India
e-mail: surekha.challa@gitam.edu

K. R. Hakeem et al. (eds.), *Essentials of Bioinformatics, Volume III*,
https://doi.org/10.1007/978-3-030-19318-8_11

Under high salinity, plants experience both osmotic and ionic stress. The salt concentrations outside the roots rise rapidly, thereby leading to inhibition of water uptake by the roots, cell expansion, and lateral bud development (Munns and Tester 2008). Ionic stress develops when excess Na^+ accumulates particularly in leaves leading to increase in leaf mortality with chlorosis and necrosis and subsequently decrease in essential cellular metabolism activities such as photosynthesis (Yeo and Flowers 1986; Glenn et al. 1999). As NaCl is the most soluble and widespread salt, all plants have evolved mechanisms to regulate its accumulation.

Under salinity stress, plant cells need to maintain low cytosolic Na^+ level and high K^+ levels, resulting in a high cytosolic K^+/Na^+ ratio that is crucial for vital cellular metabolisms (Jeschke 1984; Blumwald 2000). The strategies generally employed by plants for the maintenance of a high K^+/Na^+ ratio in the cytosol include Na^+ extrusion and/or the intracellular compartmentalization of Na^+ (mainly in the plant vacuole). These mechanisms are vital for detoxification of cellular Na^+ levels and cellular osmotic adjustment which are needed to tolerate salt stress and plant survival (Blumwald 2000; Gaxiola et al. 2001; Li et al. 2010; Wei et al. 2011). The compartmentalization of Na^+ into vacuoles prevents the deleterious effects of Na^+ in the cytosol and allows the plants to use NaCl as an osmoticum. NaCl generates an osmotic potential that drives water into the cells (Gutiérrez-Luna et al. 2018).

The plant cell vacuole performs important biological functions such as recycling of cell components, regulation of turgor pressure, detoxification of xenobiotics, and accumulation of many useful substances. A large number of vacuolar proteins are known to be involved in support of the above multifaceted functions (Ohnishi et al. 2018). They include active pumps, carriers, ion channels, receptors, and structural proteins. Several major proteins of the tonoplast have been extensively investigated, and it was found that the three most abundant proteins of the tonoplast are vacuolar H^+-ATPase (V-ATPase), H^+-pyrophosphatase (V-PPase) (Maeshima 2000, 2001; Meng et al. 2017), and water channels (aquaporins) (King et al. 2004).

V-ATPase and VPPase coexist on the plant vacuolar membrane and use ATP and inorganic pyrophosphate (PPi), respectively, as energy sources for generating an electrochemical gradient of protons across the tonoplast. This facilitates the functioning of the Na^+/H^+-antiporter. The V-ATPase enzyme is a multisubunit proton pump found in all eukaryotes consisting of the peripheral (V1) complex responsible for ATP hydrolysis and the membrane-integral (Vo) complex responsible for proton translocation. V-ATPase is the largest complex in the tonoplast, with a total molecular size of about 750 kDa.

VPPase is a heat stable single polypeptide found in plants, algae, photosynthetic bacteria, protozoa, and archaebacteria (Rea et al. 1992; Maeshima 2000). It functions as a tonoplast proton pump and helps in Na^+ compartmentation. In plants, two isoforms of VPPase have been identified; one is potassium-dependent, while the other is potassium-independent (Belogurov and Lahti 2002; Schilling et al. 2017). Aquaporins are referred to as intercellular water channels imbedded in the membranes, and they facilitate transport of water, small solutes, and ions across membranes (Aharon et al. 2003; Porcel et al. 2005).

In this chapter, the vacuolar transporter VPPase has been reviewed with respect to its structure, function, phylogeny, and mode of action. This provides us with an understanding how plants tolerate and survive under salt-stressed environments.

11.2 Molecular Phylogeny of VPPase

VPPases have been reported to be highly conserved among land plants and less among archaeon, protozoan, and bacteria (Suneetha et al. 2016). VPPase from *R. rubrum* (Baltscheffsky et al. 1998), *Acetabularia acetabulum* (marine algae) (Ikeda et al. 1999), and *Chara coralline* (green algae) (Nakanishi et al. 1999) predicted the overall identities of amino acid sequences among these three phylogenetically separated organisms. It was reported that *R. rubrum* PPase synthase (660 residues) exhibited 36–39% with V-PPases of land plants and 40% with *A. acetabulum* V-PPase. Moreover *A. acetabulum* V-PPase shared 47% identity with land plant VPPases. However, the highest identity was observed in case of *C. corallina* (71%) with respect to land plants. These observations of sequence similarity suggest that *C. corallina* is evolutionarily closer to land plant than *R. rubrum* and *A. acetabulum*. Phylogeny with respect to other land plants revealed that VPPase of *A. thaliana* (AtVPP), *H. vulgare* (HvVPP), *B. vulgaris* (BvVPP), *N. tabacum* (NtVPP), and *O. sativa* (OsVPP) ranged from 761 to 771 amino acids in length. The amino acid sequences were found to be highly conserved with 86–91% sequence similarity among the land plants.

Phylogeny is used in establishing the origin and evolution pattern of a gene of particular species with respect to the other species. Generally phylogenetic tree is constructed using neighbor-joining (NJ) or maximum parsimony (MP) or maximum likelihood (ML) method (Saitou and Nei 1987). Suneetha et al. (2016) carried out phylogenetic studies on land plants, archaea, and bacterial V-PPases (Fig. 11.1).

Suneetha (2015) generated three phylogenetic trees in land plants using NJ, MP, and ML which showed similar topologies in both distance and character methods but differed in their branching order. Topological similarity of the trees obtained by different methods (NJ, MP, and ML) indicates that these clusters are not incidental and branching order reflected the expected pattern in all plants. The MP tree was constructed from 772 characters, out of which 515 were observed as conserved and 255 were variable, and of these 183 were parsimony informative. The tree length (L), consistency index (CI), and retention index (RI) in land plants were found to be 677, 0.61, and 0.77. The ML tree has a significant maximum likelihood tree length (−6594.00) (Fig. 11.2).

Similarly, Liu et al. (2011) reported that VPPase isolated from *Suaeda corniculata* showed highest similarity with *Kalidium foliatum* (96%), *Suaeda salsa* (94%), *Chenopodium rubrum* (89%), *Beta vulgaris* (89%), *Chenopodium glaucum* (88%), and *Arabidopsis thaliana* (87%). Dong et al. (2011) reported that apple VPPase (MdVHP1) shared highest similarity with peach VPPase (94%) followed by 87% similarity with VPPases of tobacco, grapevine, and *Arabidopsis.* Similarly, VPPase

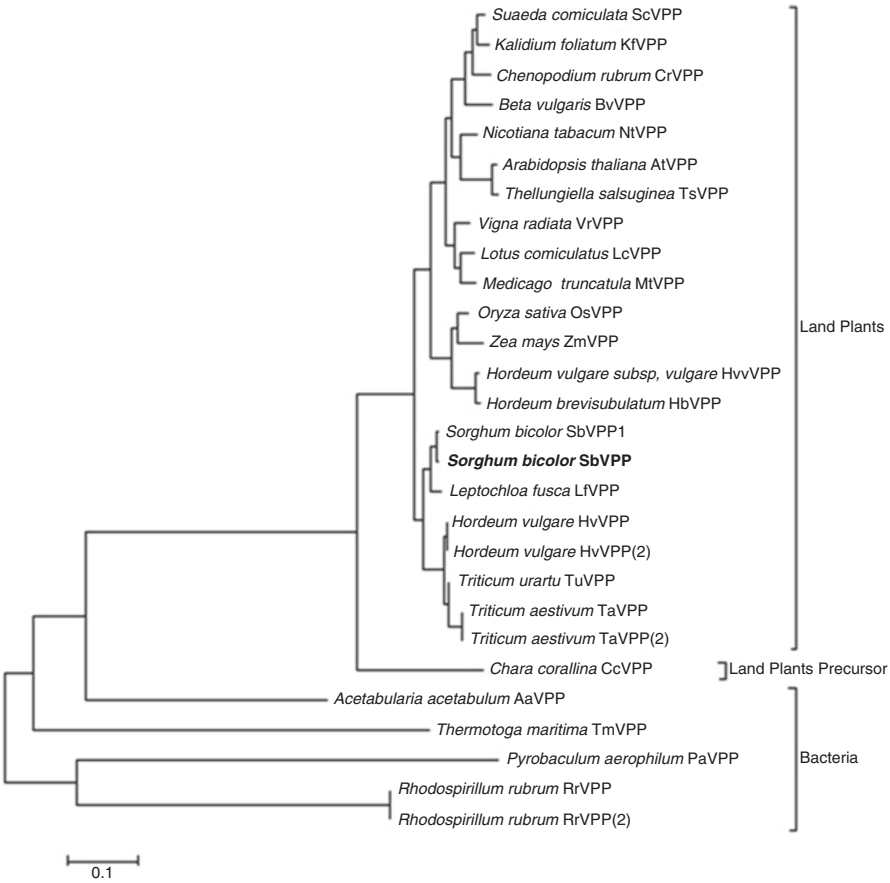

Fig. 11.1 Relationship of 28 VPPases among land plants, land plant precursor, and bacteria as represented in a phylogenetic tree. (Source: Suneetha et al. 2016)

of *H. caspica* showed high sequence similarity with VPPases from Chenopodiaceae family and shared 95% sequence identity with VPPase of *K. foliadum*. All the studies reported the evolutionary history and relationship of VPPase gene among bacteria, land plants, and its precursor. The studies also provided enough evidence to conclude that VPPase gene is highly conserved among plant family members.

11.3 Motifs of VPPase

The structural model of VPPase showing N- and C-terminals in vacuolar end, transmembrane helices, and three conserved regions (CS1, CS2, and CS3) was reported by Maeshima (2001). Immunochemical analysis confirmed that these conserved sequences are located in the cytosolic loops (Takasu et al. 1997).

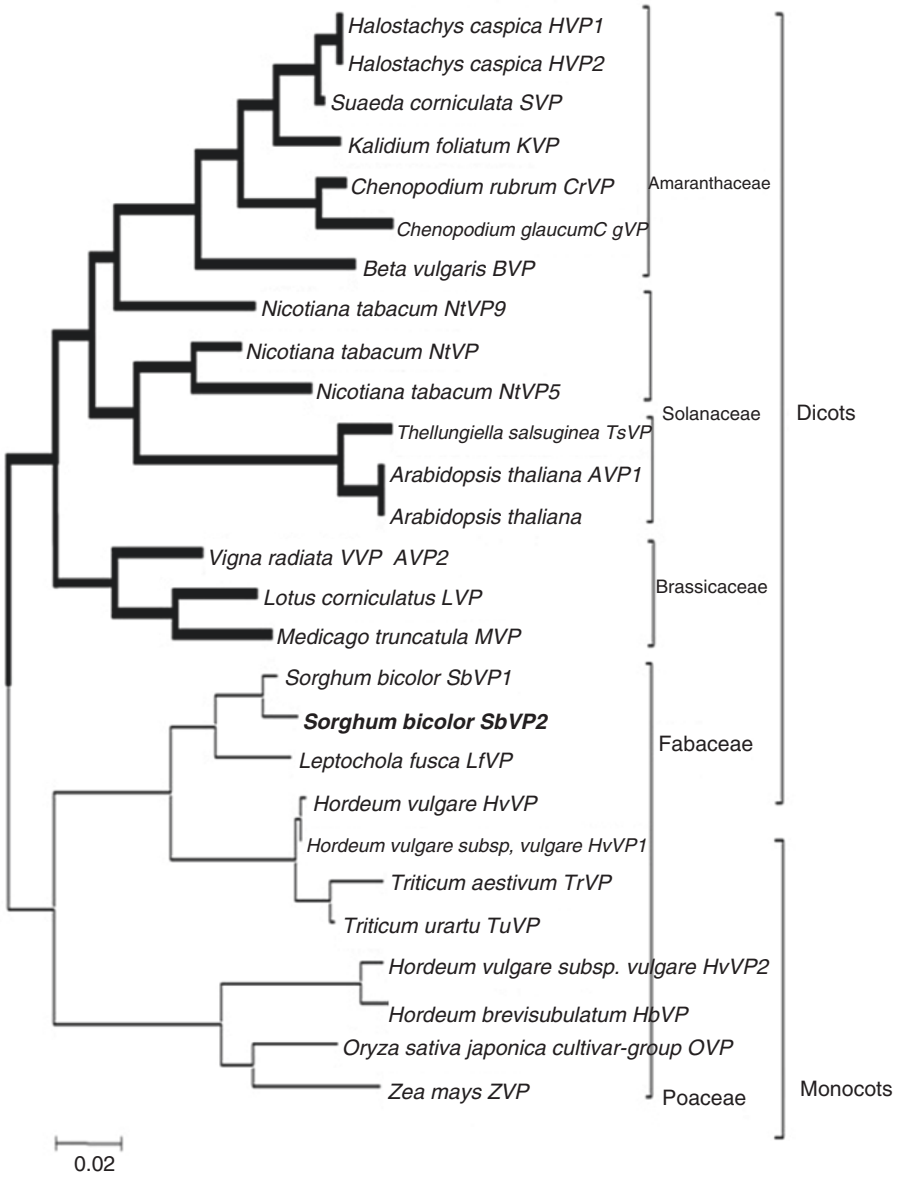

Fig. 11.2 Relationship of VPPases among land plants. The phylogenetic tree was generated using maximum likelihood method. (Source: Suneetha 2015)

Comparison of all VPPase genes from *C. coralline*, *A. acetabulum*, *R. rubrum*, and land plants reported with three highly conserved regions called motifs. The conserved motifs have been designated as CS1, CS2, and CS3 motifs (Rea and Poole 1993; Baltscheffsky et al. 1999; Maeshima 2000; Mimura et al. 2004; Suneetha 2015). Plant VPPase are characterized by the presence of cytosolic loops

(CLs), vacuolar loops (VLs), and transmembrane domains (TMDs) besides the N- and C-terminals residues (Zhen et al. 1997). Site-directed mutagenesis and immunochemical analysis revealed that the cytosolic domains are more conversed than the vacuolar domains and thus are crucial for VPPase enzyme activity.

The first conserved segment (CS1) has consensus sequence of DVGADLVGKVE and functions as the catalytic domain for substrate hydrolysis (Rea and Poole 1993; Schocke and Schink 1998). In addition to the catalytic site, there are binding sites for Mg^{2+}, K^{+}, and reagents, such as *N*,*N*-dicyclohexylcarbodiimide (DCCD), 7-chloro-4-nitrobenzo-2-oxa- 1,3-diazole (NBDCl), and *N*-ethylmaleimide (NEM) (Maeshima 2000; Sanders et al. 1999). Fukuda et al. (2004) validated the presence of NEM binding site at Cys-635 position, and Glu-306, Asp-505, and Glu-752 positions were identified as DCCD binding residues in barley. Zhen et al. (1997) conducted mutation and biochemical assays and revealed that Glu305 and Asp504 of *A. thaliana* V-PPase directly participate in DCCD binding and are presumably critical for catalysis.

The second conserved segment (CS2) is highly conserved and is located in a hydrophilic loop in the cytosol end. Suneetha (2015) reported that the CS2 motif has consensus sequence GSAALVSL and is approximately located at amino acid positions 543–550 in *Sorghum bicolor*. Suneetha (2015) reported that CS2 motif has function similar to rhodopsin like G-protein-coupled receptors (GPCRs) and is equipped with unique calcium signaling signature property that senses the high cytosolic Ca^{2+} levels and initiates V-PPase activity.

The third conserved segment (CS3) is located in the carboxyl-terminal part and contains 12 charged residues. It has consensus sequence GDTIGD exposed to the cytosol and plays a critical role in catalytic function in association with CS1 and CS2 segments (Liu et al. 2011; Rea et al. 1992). The position of these conserved regions change from one plant VPPase to others. For example, CS1 functional motifs DDPR and VGDN are located at 271 and 285 amino acid positions in mung bean, whereas in *S. corniculata* they are located at 266 and 280 amino acid positions, and in *S. bicolor* they occupy the 266 and 281 amino acid positions (Fig. 11.3). Similarly, the other conserved sequences CS2 and CS3 motifs are also highlighted in amino acid sequence alignment.

11.4 Structure of VPPase

Vacuolar H^{+}-pyrophosphatase (VPPase) catalyzes electrogenic H^{+}-translocation from the cytosol to the vacuolar lumen at the expense of hydrolysis of inorganic pyrophosphate (PPi). PPi is produced as a by-product of several metabolic processes, such as polymerization of DNA and RNA and synthesis of aminoacyl-tRNA (protein synthesis), ADP-glucose (starch synthesis), UDP-glucose (cellulose synthesis), and fatty acyl- CoA (L-oxidation of fatty acid).

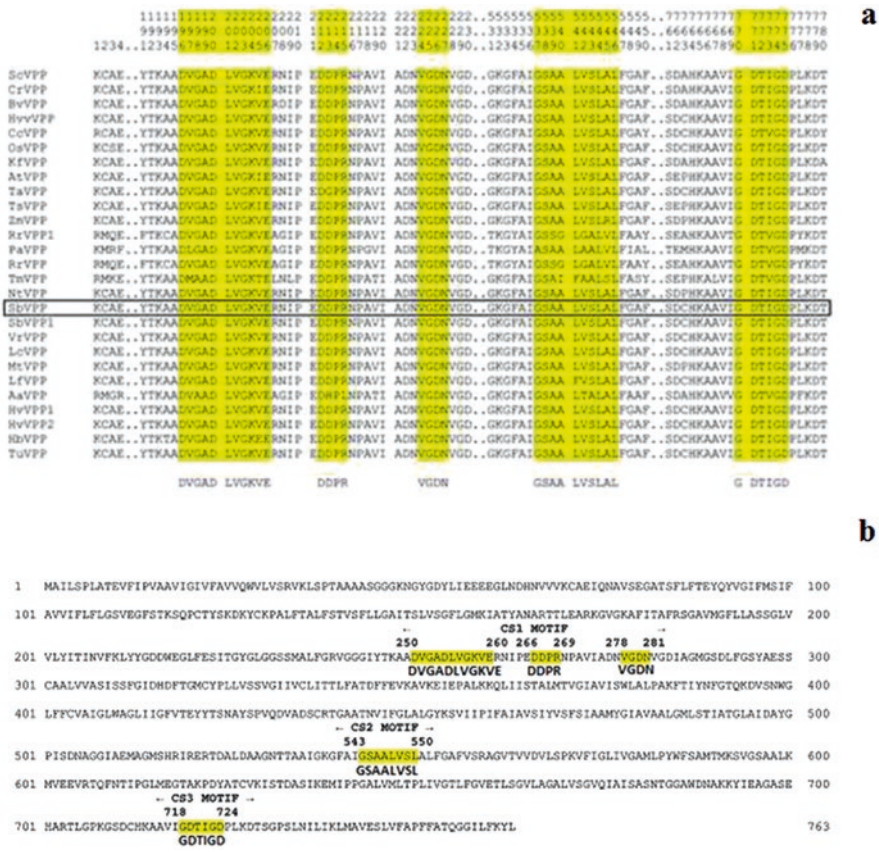

Fig. 11.3 Three conserved motifs CS1, CS2, and CS3 highlighted in (**a**) amino acid alignment are generated for sequences of VPPases; (**b**) region of conserved sequences of CS1, CS2, and CS3 are highlighted taking *S. bicolor* VPPase (meta-analysis of motifs was carried out)

11.4.1 Topology

VPPase consists of a single polypeptide, and its substrate, inorganic pyrophosphate (PPi), is one of the simplest high-energy compounds (Baltscheffsky et al. 1999; Maeshima 2000; Rea and Poole 1993). V-PPase gene encodes a polypeptide with 761–771 amino acids. Various V-PPase genes have been analyzed from different plant and bacterial species (Table 11.1). It was reported that VPPase gene isolated from *H. capsica* encodes 764 amino acids, apple VPPase gene encodes 771 amino acids, *S. corniculata* encodes 764, and *S. bicolor* encodes 763 amino acids.

Hydropathic and membrane topological analyses indicated that VPPase in general consists of 4–17 transmembrane domains (Table 11.2). Suneetha (2015) predicted that *S. bicolor* VPPase has 16 transmembrane regions using TMpred and

Table 11.1 List of VPPase genes and corresponding transmembrane helices

Sl no	Plant species	Accession ID	Transmembrane helices		No. of amino acids	References
			I → O	O → I		
1	*Arabidopsis thaliana* L.	BAA32210	14	14	770	Sarafian et al. (1992)
		AAF31163	17	16	800	
		AAG09080	17	16	802	
2	*Beta vulgaris* L.	AAA61609	13	14	761	Kim et al. (1994a, b)
		AAA61610	14	15	765	
3	*Vigna radiata* L.	P21616	14	13	766	Nakanishi and Maeshima (1998)
4	*Cucurbita moschata*	BAA33149	14	14	768	Maruyama et al. (1998)
5	*Nicotiana tabacum* L.	Q43797	13	13	766	Lerchl et al. (1995)
		Q43798	13	15	765	
6	*Oryza sativa* L.	BAA08232	14	15	771	Sakakibara et al. (1996)
		BAA31524	15	16	767	
7	*Hordeum vulgare* L.	BAA02717	14	15	762	Tanaka et al. (1993)
8	*Triticum aestivum* L.	AAP55210	14	15	762	Brini et al. (2005)
9	*Cucumis sativus* L.	ABN48304	3	3	161	Kabala et al. (2008)
10	*Vitis vinifera* L.	NP001268155	14	14	764	Da Silva et al. (2013)
		CAD89675	14	14	764	Venter et al. (2006)
11	*Medicago truncatula*	AES91661	12	14	624	Young et al. (2011)
		AES91660	13	14	765	
		KEH28512	17	17	799	
12	*Triticum urartu*	EMS67279	9	9	414	Ling et al. (2013)
		EMS65629	14	15	762	
		EMS53286	14	14	700	
13	*Zea mays* L.	NP001168714	1	1	97	Schnable et al. (2009)
		AFW77254	13	15	765	
		AFW70478	13	15	766	
14	*Salicornia europaea* L.	AEI17666	14	15	763	Lv et al. (2012)
		AEI17665	14	14	764	
15	*Aeluropus littoralis*	ALO51665	14	16	763	Ebrahimi et al. (2015)
16	*Ipomoea babatas* L.	AFQ00710	13	14	767	Fan (2011)
17	*Oxybasis rubra* L.	AAM97920	14	14	764	Kranewitter et al. (2002)
18	*Sorghum bicolor* L.	ACV74424	15	16	763	Anjaneyulu et al. (2014)

(continued)

Table 11.1 (continued)

Sl no	Plant species	Accession ID	Transmembrane helices		No. of amino acids	References
			I → O	O → I		
19	*Solanum lycopersium* L.	NP_001307479	14	15	767	Mohammed et al. (2012)
		BAM65603	13	13	765	
		BAM65604	17	16	800	
20	*Kalidium foliatum*	ABK91685	14	14	764	Yao et al. (2012)
21	*Chara corallina*	AB018529	15	16	793	Nakanishi et al. (1999)
22	*Acetabularia acetabulum*	D88820	13	14	721	Ikeda et al. (1999)
23	*Rhodospirillum rubrum*	AF044912	14	15	660	Baltscheffsky et al. (1998)

Table 11.2 Sequence positions of possible transmembrane helices from inside to outside and vice versa in VPPase of *S. bicolor*

Inside to outside helices				Outside to inside helices			
From	To	Score	Centre	From	To	Score	Centre
11(14)	31 (28)	2024	221	11 (14)	31 (28)	2589	21
95 (95)	111 (111)	2670	104	92 (92)	111 (108)	2664	101
136 (138)	156 (153)	2054	146	136 (136)	156 (156)	2109	146
188 (188)	206 (204)	2150	197	188 (191)	206 (206)	2147	198
229 (229)	244 (244)	682	236	223 (227)	244 (242)	860	234
296 (296)	314 (310)	1049	303	293 (293)	314 (309)	1058	302
325 (325)	342 (342)	2139	335	326 (326)	342 (342)	2143	333
366 (366)	383 (383)	1886	373	361 (361)	381 (379)	1974	372
401 (401)	417 (415)	2725	408	401 (402)	418 (418)	2629	409
456 (460)	476 (476)	2120	467	456 (456)	475 (475)	2120	466
476 (476)	494 (490)	1990	483	471 (473)	490 (488)	1997	481
539 (541)	557 (557)	2092	550	539 (542)	557 (557)	1991	549
573 (573)	589 (589)	1938	581	572 (572)	588 (588)	1672	581
644 (644)	659 (659)	1324	652	639 (642)	659 (657)	1609	649
661 (661)	681 (678)	1216	669	661 (664)	680 (678)	1256	671
740 (743)	760 (757)	1314	750	740 (740)	760 (757)	1238	750

TMHMM. The results obtained showed that the sequences has 16 inside to outside helices orientations and 16 outside to inside helices orientations of the transmembranes (Fig. 11.4a, b).

The 3D structure of VPPase is a vacuolar membrane-bound protein compactly folded in rosette manner in two concentric walls (Lin et al. 2012; Suneetha et al. 2016; Suneetha 2015) (Fig. 11.5). Lin et al. (2012) reported that mung bean VPPase has 16 transmembrane helices, but it exists as a homodimer, and Suneetha (2015)

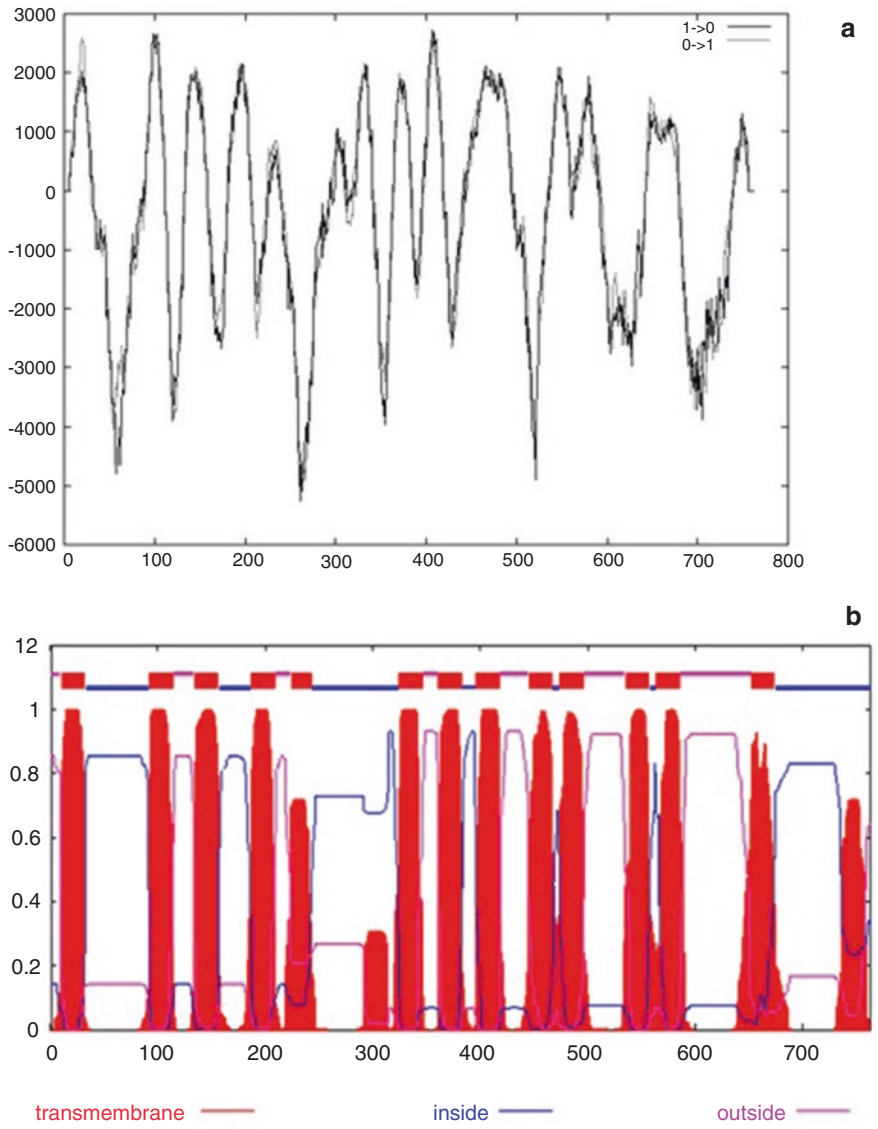

Fig. 11.4 Transmembrane helices of VPPase in *S. bicolor* (**a**) TM pred, (**b**) TMHMM. (Source: Suneetha 2015)

reported that *S. bicolor* VPPase exists as monomer with 16 transmembrane helices. The core has six transmembrane helices surrounded by ten transmembrane helices which form the inner and outer walls of the pump which is displayed in cylinders (Fig. 11.6). Two short helices are present on the cytosolic side; two helices and two antiparallel β-strands are present on the luminal side of the protein (Fig. 11.7).

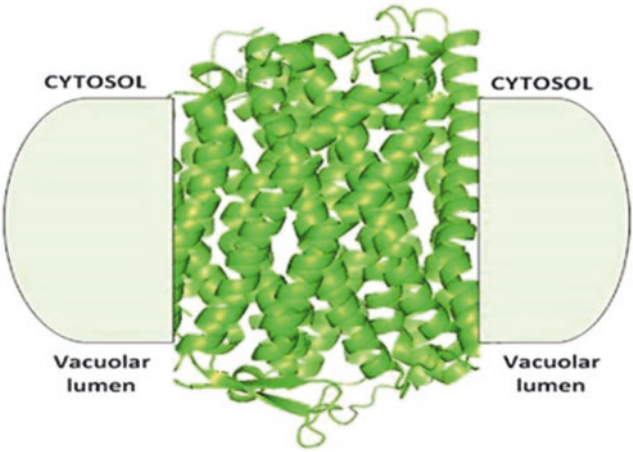

Fig. 11.5 VPPase protein compactly folded as membrane-bound protein. (Source: Suneetha et al. 2016)

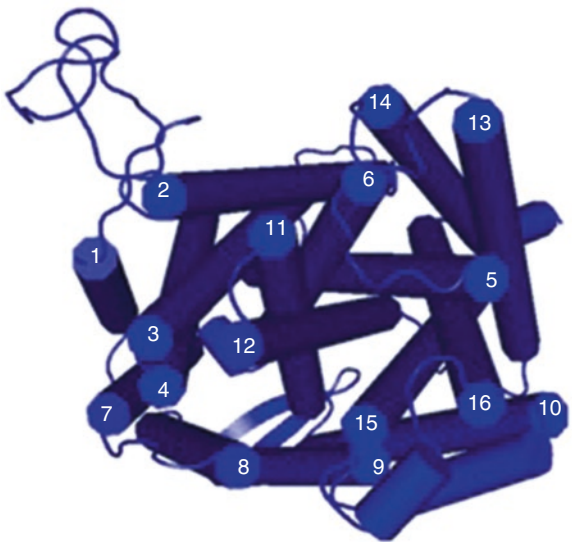

Fig. 11.6 Sixteen transmembrane helices (blue cylinders) with six helices in the core surrounded by ten transmembrane helices to form inner and outer walls of the pump. (Source: Suneetha 2015)

The core of the model has one IDP molecule surrounded by five Mg^{2+} ions which are essential for the activity of V-PPases and one K^+ ion which acts as stimulator (Fig. 11.8). The above elements are highly conserved among the VPPases which forms a hydrophobic door to the hydrophilic surroundings of the vacuolar lumen. The hydrophobic gate prevents the reflux of H^+ ions and helps in maintaining the translocation of H^+ from cytosol to vacuolar lumen (Fig. 11.9). The space-fill representation of VPPase model is considered to analyze electrostatic surface potential.

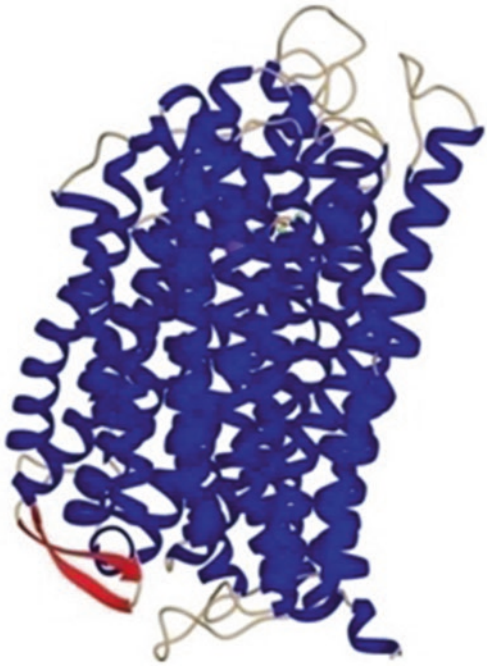

Fig. 11.7 Ribbon structure of VPPase containing 16 transmembrane helices (colored in blue) and antiparallel β-strands (colored in red). (Source: Suneetha 2015)

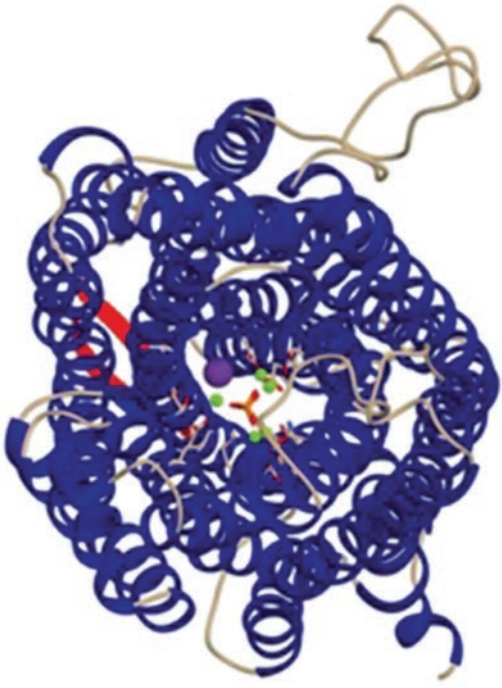

Fig. 11.8 VPPase model of *S. bicolor* rotated to 600 to visualize the core with one imidodiphosphate (IDP), five Mg2+ (colored in green), and one K+ ions (colored in purple). (Source: Suneetha 2015)

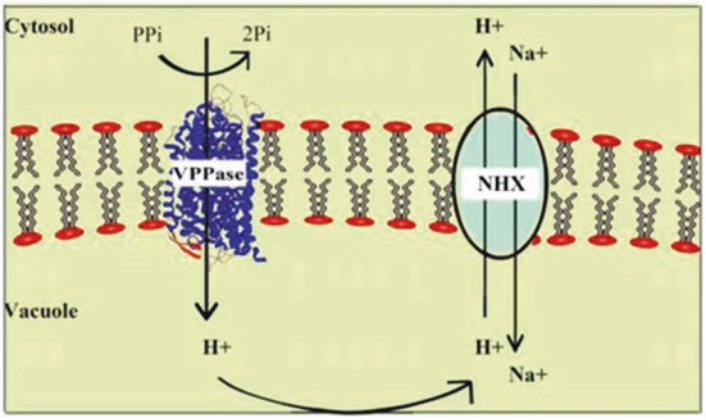

Fig. 11.9 Working model of the VPPase showing the pumping of protons into vacuole to generate electrochemical gradient against which sodium is taken in under stress conditions. (Source: Suneetha 2015)

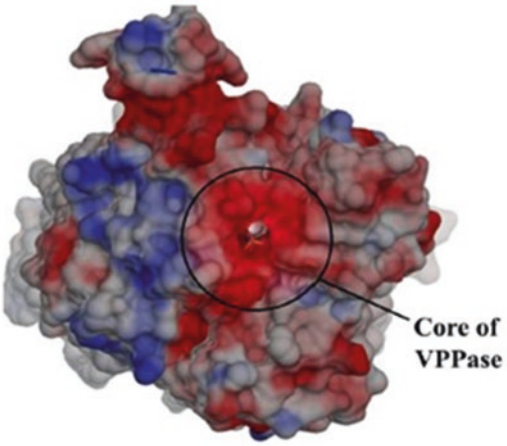

Fig. 11.10 The space-fill representation of modeled VPPase showing electrostatic surface potential. The electrostatic surface negative potential (red), positive (blue), and neutral (white) are represented. The core of the model contains IDP binding site. (Source: Suneetha 2015)

The surface potential is indicated by colors as in Fig. 11.10. The core of model which contains IDP binding site is represented within the circle the core of VPPase (Fig. 11.10).

11.4.2 Metal Geometry

V-PPase requires free Mg^{2+} as an essential cofactor. $MgCl_2$ and $MgSO_4$ are added to the buffers for solubilization and purification of the enzyme during its isolation (Maeshima and Yoshida 1989; Britten et al. 1989; Rea and Poole 1986). Binding of

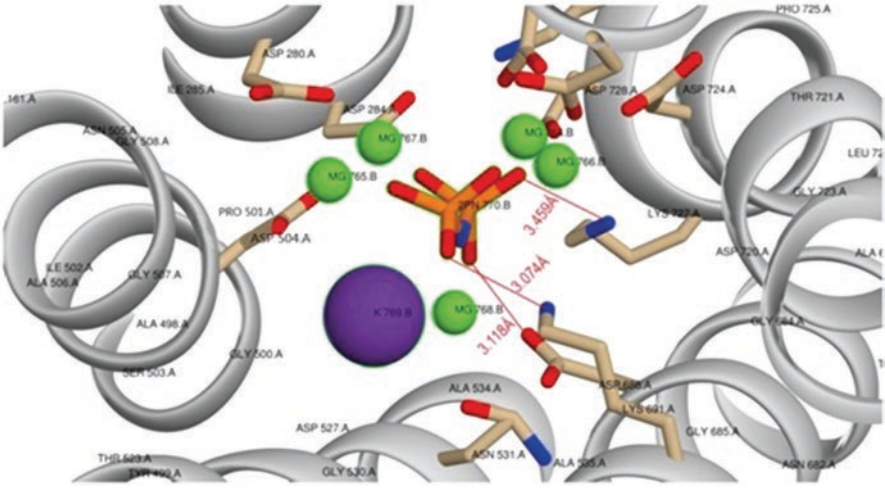

Fig. 11.11 The core of VPPase showing coordinating amino acids from IDP molecule to five Mg2+ ions. (Source: Suneetha 2015)

Mg^{2+} stabilizes and activates the enzyme. Baykov et al. (1993) reported the presence of high-affinity and low-affinity Mg^{2+} binding sites of mung bean. Binding of Mg^{2+} to VPPase not only activates the enzyme but also protects it from heat inactivation (Baykov et al. 1993). Suneetha (2015) reported that the core has five Mg^{2+} and one K^+ ions along with one IDP which play an important role in activating VPPases by transphosphorylation reaction involving ATP's. Each Mg^{2+} ion interacts with surrounding amino acids like aspartic acid, asparagines, and glutamic acid (Fig. 11.11). Potassium ion acts as stimulator of VPPase and is surrounded by amino acids like asparagine and glycine. K^+ stimulates VPPase activity by more than threefold in most cases (Gordon-Weeks et al. 1999). The maximal activity of VPPase was obtained in the presence of more than 30 mM KCl in most cases. Suneetha (2015) also reported that there are eleven phosphate binding sites represented in yellow color balls and interacting residues with green color (Fig. 11.12).

11.4.2.1 Regulation of VPPase Enzyme Activity

Studies on VPPase from various plant species revealed the relationship between the enzyme activity of the proton pump with respect to varying concentrations of cytosolic ions and chemical compounds. K^+ ions have been associated with increased VPPase enzyme activity in *A.thaliana* type 2 VPPase (AVP2). Ca^{2+} reversibly inhibits VPPase activity through formation of Ca-PPi which is a strong, competitive inhibitor for the soluble PPases (Baykov et al. 1999). Changes in free cytosolic Ca^{2+} levels have also been associated with negative inhibition of VPPase activity in bean guard cells (Darley et al. 1998) and barley (Swanson and Jones 1996).

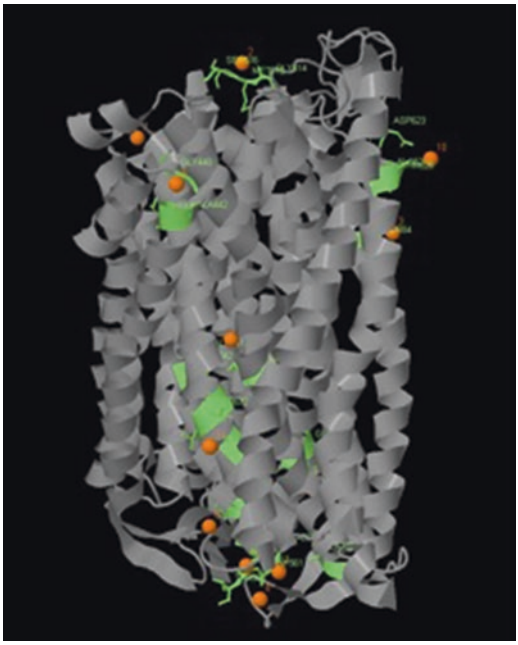

Fig. 11.12 Eleven phosphate binding sites of VPPase are represented in yellow colored balls and interacting residues in green color. (Source: Suneetha 2015)

Cytosolic Mg^{2+} concentration has also been reported for optimum enzyme activity in *S. bicolor*, mung bean, and barley. Moreover excessive Na^{+} concentrations have been reported to inhibit enzyme activity in red beet (Rea and Poole 1985).

Among the artificial substances tested, it reported that amino methylene bisphosphonate (AMBP) is a potent inhibitor of VPPase in mung bean and *A. thaliana* VPPase AVP2 and AVP1 (Zhen et al. 1994). The effectiveness of bisphosphonates as an inhibitor of VPPase was carried out, and it was concluded that a nitrogen atom in the carbon chain of bisphosphonates increased the inhibitory effect of the enzyme (Gordon-Weeks et al. 1999).

11.5 VPPase and Its Activity

Proton pump VPPase gets activated upon signals perceived by plants. The sequences of events occurring during the activation of proton pump are as follows:

Abiotic stress (high salinity, drought, high temperatures, etc.) in plants is perceived by root tissues and cells. The cells activate receptor-bound G-proteins to activate protein kinases by the breakdown of membrane-bound phosphatidylinositol bisphosphate (PIP2) to diacylglycerol (DAG) and inositol triphosphate (IP3) (Mahajan and Tuteja 2005; Tuteja 2007). IP3 induces endoplasmic reticulum in release of Ca^{2+} and other side; it also makes calcium channels to open to increase intracellular Ca^{2+} levels. CS1 and CS3 motifs form the core catalytic domain and are

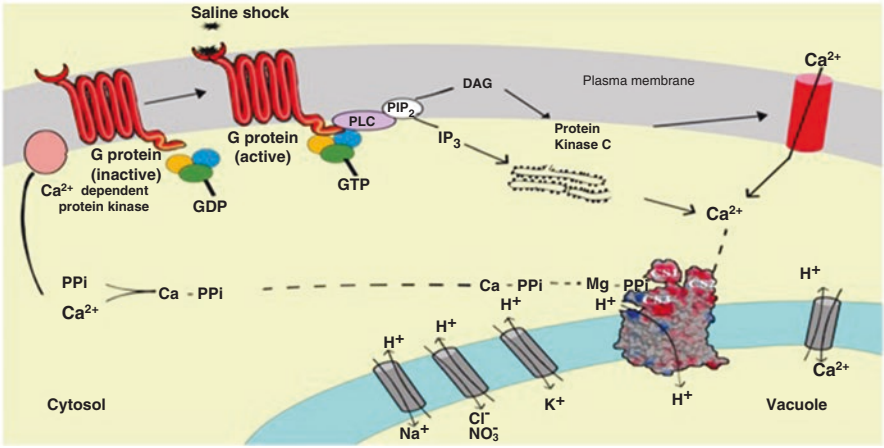

Fig. 11.13 Web of events which show saline shock initiating cascade of signals to generate PMF that drives sodium into vacuole leading to salt tolerance in plants

essential for hydrolyzing PPi and transport protons (Fig. 11.13). CS2 motif of VPPase, similar to rhodopsin-like G-protein-coupled receptor (GPCR) with calcium signaling signature property, senses these high cytosolic Ca^{2+} levels and transduces extracellular signal. The free available cytosolic Ca^{2+} may be phosphorylated to Ca-PPi by Ca^{2+}-dependent membrane-bound protein kinase and PPi (Johannsen et al. 1996). The substrate PPi of Ca-PPi is exchanged with Mg^{2+} to form Mg-PPi at the core catalytic site from CS1 and CS3.

The above elements are highly conserved among the VPPases that form hydrophobic door to the hydrophilic surroundings of vacuolar lumen. The acidic residues in the core catalytic site help in PPi hydrolysis and proton transport into vacuole. The hydrophobic gate prevents the reflux of H^+ ions and helps in maintaining the translocation of H+ from cytosol to vacuolar lumen. The pumping of H^+ into vacuole builds electrochemical gradient (proton motive force, PMF) which changes its pH (2–4 pH units, equivalent to −120 to –240 mV) (Isayenkov et al. 2010). The PMF can energize various antiporters such as Na^+ and K^+: H^+ exchanger, NO_3^- and Cl^-: H^+ exchanger, etc. resulting in influx of Na^+, K^+, NO_3^-, and Cl^- from cytosol to vacuole. This influx reduces the toxicity of cytosol to protect the cell against deleterious effects thus caused due to abiotic stress. Therefore, overall signaling web plays an important role in providing stress tolerance to plants.

11.6 Conclusion

Vacuolar transporters are vital components of cellular network. They enable the plant to respond to the changing environmental conditions, store nutrients and energy during surplus production, and maintain optimal metabolic conditions in the

cytosol. Plant vacuolar VPPase, a model of proton pump, is considered as integral enzyme due to its structure-function relationship.

Structural analysis using both laboratory and bioinformatic approaches revealed the functional domains along with the conserved segments (CS1, CS2, and CS3) that play an active role in the translocation of H^+ ions into the vacuole from the cytosol. Phylogenetic analysis of all known VPPase across land plants, archaea, protozoan, and bacteria increased our knowledge of the tonoplast dramatically over the past decade. Studies established that during evolution of organisms, ancestral plant species obtained VPPase in addition to vacuolar-type V-ATPase.

However, more information is required on protein-ligand interactions and the molecular evolution of VPPase. It has been reported that the expression levels of VPPase change according to the physiological conditions and in response to environmental stresses. However, the regulatory mechanism and the posttranslational regulations of VPPase are yet to be studied. Thus, these analyses are extremely important toward establishing the role of VPPase as effective proton pump dedicated toward alleviating salt stress. The VPPase gene has been successfully used to engineer transgenic plants. Overexpression of the VPPase gene was able to confer effective Na^+ compartmentation into the vacuole. Moreover, various VPPase from other species can be isolated to study their functional properties and development of transgenic plants. Thus enabling the plant to survive during salt stress and maintain an optimum osmoticum of the cytosol.

Acknowledgments The authors are grateful to Gandhi Institute of Technology and Management (GITAM) deemed-to-be-university, for providing necessary facilities to carry out the research work and for extending constant support in writing this review.

References

Aharon R, Shahak Y, Wininger S, Bendov R, Kapulnik Y, Galili G (2003) Overexpression of a plasma membrane aquaporin in transgenic tobacco improves plant vigor under favorable growth conditions but not under drought or salt stress. Plant Cell 15:439–447

Anjaneyulu E, Reddy PS, Sunita MS, Kishor PBK, Meriga B (2014) Salt tolerance and activity of antioxidative enzymes of transgenic finger millet overexpressing a vacuolar H+-pyrophosphatase gene (SbVPPase) from *Sorghum bicolor*. J Plant Physiol 171(10):789–798

Ashraf M, Athar HR, Harris PJC, Kwon TR (2008) Some prospective strategies for improving crop salt tolerance. Adv Agron 97:45–110

Baltscheffsky M, Nadanaciva S, Schultz A (1998) A pyrophosphate synthase gene: molecular cloning and sequencing of the cDNA encoding the inorganic pyrophosphate synthase from *Rhodospirillum rubrum*. Biochim Biophys Acta 1364:301–306

Baltscheffsky M, Schultz A, Baltscheffsky H (1999) HC-PPases: a tightly membranebound family. FEBS Lett 457:527–533

Baykov AA, Bakuleva NP, Rea PA (1993) Steady-state kinetics of substrate hydrolysis by vacuolar H+-pyrophosphatase: a simple three-state model. Eur J Biochem 217:755–762

Baykov AA, Cooperman BS, Goldman A, Lahti R (1999) Prog Mol Subcell Biol 23:127–150

Belogurov GA, Lahti R (2002) A lysine substitute for K+-A460K mutation eliminates K+ dependence in H+-pyrophosphatase of Carboxydothermus hydrogenoformans. J Biol Chem 277:49651–49654

Blumwald E (2000) Sodium transport and salt tolerance in plants. Curr Opin Cell Biol 12:431–434

Brini F, Gaxiola RA, Berkowitz GA, Masmoudi K (2005) Cloning and characterization of a wheat vacuolar cation/proton antiporter and pyrophosphatase proton pump. Plant Physiol Biochem 43(4):347–354

Britten CJ, Turner JC, Rea PA (1989) Identification and purification of substrate-binding subunit of higher plant H+-translocating inorganic pyrophosphatase. FEBS Lett 256:200–206

Da Silva C, Zamperin G, Ferrarini A, Minio A, Dal Molin A, Venturini L, Buson G, Tononi P, Avanzato C, Zago E, Boido E (2013) The high polyphenol content of grapevine cultivar tannat berries is conferred primarily by genes that are not shared with the reference genome. Plant Cell 25(12):4777–4788

Darley CP, Skiera LA, Northrop FD, Sanders D, Davies JM (1998) Tonoplast inorganic pyrophosphatase in Vicia faba guard cells. Planta 206:272–2777

Dong QL, Liu DD, An XH, Hu DG, Yao YX, Hao YJ (2011) MdVHP1 encodes an apple vacuolar H+-PPase and enhances stress tolerance in transgenic apple callus and tomato. J Plant Physiol 168(17):2124–2133

Ebrahimi A, Monfared SRA, Kashkooli AB (2015) Pyrophosphate-energized vacuolar membrane proton pump [*Aeluropus littoralis*] agronomy and plant breeding, Tehran University, Karaj, Alborz 31587-1167, Iran

Fan W (2011) Overexpression of the Na^+/H^+ antiporter gene from sweet potato. Cassava and sweetpotato biotechnology, direct submission to NCBI with accession no. AFQ00710

Fukuda A, Chiba K, Maeda M, Nakamura A, Maeshima M, Tanaka Y (2004) Effect of salt and osmotic stresses on the expression of genes for the vacuolar H^+-pyrophosphatase, H^+-ATPase subunit A, and Na^+/H^+ antiporter from barley. J Exp Bot 55(397):585–594

Gaxiola RA, Li J, Undurraga S, Dang LM, Allen GJ, Alper SL, Fink GR (2001) Drought-and salt-tolerant plants result from overexpression of the *AVP1* H+-pump. Proc Natl Acad Sci U S A 98(20):11444–11449

Glenn EP, Brown JJ, Blumwald E (1999) Salt tolerance and crop potential of halophytes. Crit Rev Plant Sci 18:227–255

Gordon-Weeks R, Parmar S, Davies TGE, Leigh RA (1999) Structural aspects of the effectiveness of bisphosphonates as competitive inhibitors of the plant vacuolar proton-pumping pyrophosphatase. Biochem J 337:373–377

Gutiérrez-Luna FM, Hernández-Domínguez EE, Valencia-Turcotte LG, Rodríguez-Sotres R (2018) Pyrophosphate and pyrophosphatases in plants, their involvement in stress responses and their possible relationship to secondary metabolism. Plant Sci 267:11. https://doi.org/10.1016/j.plantsci.2017.10.016. Epub 2017 Nov 8.

Ikeda M, Tanabe E, Rahman MH, Kadowaki H, Moritani C et al (1999) A vacuolar inorganic HC-pyrophosphatase in *Acetabularia acetabulum*: partial purification, characterization and molecular cloning. J Exp Bot 50:139–140

Isayenkov S, Isner JC, Maathuis FJM (2010) Vacuolar ion channels: roles in plant nutrition and signalling. FEBS Lett 584:1982–1988

Jeschke WD (1984) K+-Na+ exchange at cellular membranes, intracellular compartmentation of cations, and salt tolerance. Sanity tolerance in plant. Strategies for crop improvement. Wiley-Interscience Publication, New York, pp 33–76

Johansson I, Larsson C, Ek B, Kjellbom P (1996) The major integral proteins of spinach leaf plasma membranes are putative aquaporins and are phosphorylated in response to Ca+ and apoplastic water potential. Plant Cell 8:1181–1191

Kim Y, Kim EJ, Rea PA (1994a) Isolation and characterization of cDNAs encoding the vacuolar HC-pyrophosphatase of *Beta vulgaris*. Plant Physiol 106:375–382

Kim Y, Kim EJ, Rea PA (1994b) Isolation and characterization of cDNAs encoding the vacuolar H+-pyrophosphatase of *Beta vulgaris*. Plant Physiol 106(1):375–382

King LS, Kozono D, Agre P (2004) From structure to disease: the evolving tale of aquaporin biology. Nat Rev Mol Cell Biol 5:678–698

Kranewitter W, Gogarten P, Pfeiffer W (2002) Cloning and sequencing of the vacuolar proton-pumping PPase from *Chenopodium rubrum*. Direct submission to NCBI with accession no. AAM97920

Lerchl J, K¨onig S, Zrenner R, Sonnewald U (1995) Molecular cloning, characterization and expression analysis of isoforms encoding tonoplast-bound protontranslocating inorganic pyrophosphatase in tobacco. Plant Mol Biol 29:833–840

Li Z, Baldwin CM, Hu Q, Liu HB, Luo H (2010) Heterologous expression of *Arabidopsis* H^+-pyrophosphatase enhances salt tolerance in transgenic creeping bentgrass (*Agrostis stolonifera* L.). Plant Cell Environ 33(2):272–289

Lin CH, Peng PH, Ko CY, Markhart AH, Lin TY (2012) Characterization of a novel Y2 K-type dehydrin *VrDhn1* from *Vigna radiata*. Plant Cell Physiol 53:930–942

Ling HQ, Zhao S, Liu D, Wang J, Sun H, Zhang C, Fan H, Li D, Dong L, Tao Y, Gao C (2013) Draft genome of the wheat A-genome progenitor *Triticum urartu*. Nature 496(7443):87

Liu L, Wang Y, Wang N, Dong YY, Fan XD, Liu XM, Li HY (2011) Cloning of a vacuolar H^+-pyrophosphatase gene from the halophyte *Suaeda corniculata* whose heterologous overexpression improves salt, saline-alkali and drought tolerance in *Arabidopsis*. J Integr Plant Biol 53(9):731–742

Lv S, Jiang P, Chen X, Fan P, Wang X, Li Y (2012) Multiple compartmentalization of sodium conferred salt tolerance in *Salicornia europaea*. Plant Physiol Biochem 51:47–52

Maeshima M (2000) Vacuolar H^+-pyrophosphatase. Biochim Biophys Acta 1465:37–51

Maeshima M (2001) Tonoplast transporters: organization and function. Annu Rev Plant Physiol Plant Mol Biol 52:469–497

Maeshima M, Yoshida S (1989) Purification and properties of vacuolar membrane proton-translocating inorganic pyrophosphatase from mung bean. J Biol Chem 264:20068–20073

Mahajan S, Tuteja N (2005) Cold, salinity and drought stresses: An overview. Arch Biochem Biophys 444:139–158

Maruyama C, Tanaka Y, Mitsuda NT, Takeyasu K, Yoshida M, Sato MH (1998) Structural studies of the vacuolar H+-pyrophosphatase: sequence analysis and identification of the residues modified by fluorescent cyclohexylcarbodiimide and maleimide. Plant Cell Physiol 39:1045–1053

Meng L, Li S, Guo J, Guo Q, Mao P, Tian X (2017) Molecular cloning and functional characterisation of an H^+-pyrophosphatase from *Iris lactea*. Sci Rep 7(1):17779

Mimura H, Nakanishi Y, Hirono M, Maeshima M (2004) Membrane topology of the H^+-pyrophosphatase of *Streptomyces coelicolor* determined by cysteine-scanning mutagenesis. J Biol Chem 279(33):35106–35112

Mohammed SA, Nishio S, Takahashi H, Shiratake K, Ikeda H, Kanahama K, Kanayama Y (2012) Role of vacuolar H^+-inorganic pyrophosphatase in tomato fruit development. J Exp Bot 63(15):5613–5621

Munns R, Tester M (2008) Mechanisms of salinity tolerance. Annu Rev Plant Biol 59:651–681

Nakanishi Y, Maeshima M (1998) Molecular cloning of vacuolar H^+-pyrophosphatase and its developmental expression in growing hypocotyl of mung bean. Plant Physiol 116:589–597

Nakanishi Y, Matsuda N, Aizawa K, Kashiyama T, Yamamoto K et al (1999) Molecular cloning of the cDNA for vacuolar H^+-pyrophosphatase from *Chara corallina*. Biochem Biophys Acta 1418:245–250

Ohnishi M, Yoshida K, Mimura T (2018) Analyzing the vacuolar membrane (tonoplast) proteome. In: Plant membrane proteomics. Humana Press, New York, pp 107–116

Porcel R, Gomez M, Kaldenhoff R, Ruiz-Lozano JM (2005) Impairment of NtAQP1 gene expression in tobacco plants does not affect root colonisation pattern by arbuscular *mycorrhizal* fungi but decreases their symbiotic efficiency under drought. Mycorrhiza 15:417–423

Rea PA, Poole RJ (1985) Proton-translocating inorganic pyrophosphatase in red beet (Beta vulgaris L.) tonoplast vesicles. Plant Physiol 77:46–52

Rea PP, Poole RJ (1986) Chromatographic resolution of H+-translocating pyrophosphatase from H+-translocating ATPase of higher plant tonoplast. Plant Physiol 81:126–129

Rea PA, Poole RJ (1993) Vacuolar H^+ −translocating pyrophosphatase. Annu Rev Plant Physiol Plant Mol Biol 44:157–180

Rea PA, Kim Y, Sarafian V, Poole RJ, Davies JM, Sanders D (1992) Vacuolar H^+-translocating pyrophosphatase: a new category of ion translocase. Trends Biochem Sci 17(9):348–352

Rehman S, Harris PJC, Ashraf M (2005) Stress environments and their impact on crop production. Abiotic stresses: plant resistance through breeding and molecular approaches. Haworth Press, New York, pp 3–18

Saitou N, Nei M (1987) The neighbor-joining method: a new method for reconstructing phylogenetic trees. Mol Biol Evol 4:406–425

Sakakibara Y, Kobayashi H, Kasamo K (1996) Isolation and characterization of cDNAs encoding vacuolar H^+-pyrophosphates isoforms from rice (*Oryza sativa* L.). Plant Mol Biol 31:1029–1038

Sanders D, Brownlee C, Harper JF (1999) Communicating with calcium. Plant Cell 11:691–706

Sarafian V, Kim Y, Poole RJ, Rea PA (1992) Molecular cloning and sequence of cDNA encoding the pyrophosphate-energized vacuolar membrane proton pump of *Arabidopsis thaliana*. Proc Natl Acad Sci 89(5):1775–1779

Schilling RK, Tester M, Marschner P, Plett DC, Roy SJ (2017) AVP1: one protein, many roles. Trends Plant Sci 22(2):154–162

Schnable PS, Ware D, Fulton RS, Stein JC, Wei F, Pasternak S, Liang C, Zhang J, Fulton L, Graves TA, Minx P (2009) The B73 maize genome: complexity, diversity, and dynamics. Science 326(5956):1112–1115

Schocke L, Schink B (1998) Membrane-bound proton-translocating pyrophosphatase of syntrophus gentianae, a syntrophically benzoate-degrading fermenting bacterium. Eur J Biochem 256:589–594

Suneetha G (2015) Studies on *in vitro*, *in planta* and *in silico* analysis of vacuolar proton pyrophosphatase from *Sorghum bicolor* (*Sb*V-PPase) and its overexpression in *Cajanus cajan* (unpublished doctoral thesis). GITAM University, Visakhapatnam, Andhra Pradesh, India

Suneetha G, Neelapu NRR, Surekha CH (2016) Plant vacuolar proton pyrophosphatases (VPPases): structure, function and mode of action. Int J Recent Sci Res Res 7(6):12148–12152

Swanson SJ, Jones RL (1996) Gibberellic acid induces vacuolar acidification in barley aleurone. Plant Cell 8:2211–2221

Takasu A, Nakanishi Y, Yamauchi T, Maeshima M (1997) Analysis of the substrate binding site and carboxyl terminal region of vacuolar H^+-pyrophosphatase of mung bean with peptide antibodies. J Biochem 122:883–889

Tanaka Y, Chiba K, Maeda M, Maeshima M (1993) Molecular cloning of cDNA for vacuolar membrane proton-translocating inorganic pyrophosphatase in *Hordeum vulgare*. Biochem Biophys Res Commun 190:1110–1114

Tuteja N (2007) Mechanisms of high salinity tolerance in plants. Methods Enzymol 428:419–438

Venter M, Groenewald JH, Botha FC (2006) Sequence analysis and transcriptional profiling of two vacuolar H^+-pyrophosphatase isoforms in *Vitis vinifera*. J Plant Res 119(5):469–478

Wei Q, Guo YJ, Cao H, Kuai BK (2011) Cloning and characterization of an *AtNHX2*-like Na^+/H^+ antiporter gene from *Ammopiptanthus mongolicus* (Leguminosae) and its ectopic expression enhanced drought and salt tolerance in *Arabidopsis thaliana*. Plant Cell Tissue Organ Cult 105(3):309–316

Yao M, Zeng Y, Liu L, Huang Y, Zhanq F (2012) Overexpression of the halophyte *Kalidium Foliatum* H^+-pyrophosphatase gene confers salt and drought tolerance in *Arabidopsis thaliana*. Mol Biol Rep 39(8):7989–7996

Yeo AR (1999) Predicting the interaction between the effects of salinity and climate change on crop plants. Sci Hortic 78:159–174

Yeo AR, Flowers TJ (1986) The physiology of salinity resistance in rice (*Oryza sativa* L.) and a pyramiding approach to breeding varieties for saline soils. Aust J Plant Physiol 13:75–91

Young ND, Debellé F, Oldroyd GE, Geurts R, Cannon SB, Udvardi MK, Benedito VA, Mayer KF, Gouzy J, Schoof H, Van de Peer Y (2011) The *Medicago* genome provides insight into the evolution of rhizobial symbioses. Nature 480(7378):520

Zhen RG, Baykov AA, Bakuleva NP, Rea PA (1994) Aminomethylenediphosphonate: a potent type-specific inhibitor of both plant and phototrophic bacterial H+-pyrophosphatases. Plant Physiol 104:153–159

Zhen RG, Kim EJ, Rea PA (1997) Acidic residues necessary for pyrophosphate-energized pumping and inhibition of the vacuolar H^+-pyrophosphatase by N, N′-dicyclohexylcarbodiimide. J Biol Chem 272:22340–22348